Front. Phys. 11(2), 117401 (2016)
DOI 10.1007/s11467-015-0527-4

RESEARCH ARTICLE

Magnetic order driven by orbital ordering in the semiconducting $KFe_{1.5}Se_2$

Qing Jiang, Dao-Xin Yao[†]

State Key Laboratory of Optoelectronic Materials and Technologies, School of Physics and Engineering, Sun Yat-sen University, Guangzhou 510275, China

Corresponding author. E-mail: [†]*yaodaox@mail.sysu.edu.cn*

Received September 7, 2015; accepted November 2, 2015

The two-orbital Hubbard model is studied numerically by using the Hartree-Fock approximation in both real space and momentum space, and the ground-state properties of the alkali metal iron selenide semiconducting $KFe_{1.5}Se_2$ are investigated. A rhombus-type Fe vacancy order with stripe-type antiferromagnetic (AFM) order is found, as was observed in neutron scattering experiments [J. Zhao, et al., *Phys. Rev. Lett.* 109, 267003 (2012)]. Hopping parameters are obtained by fitting the experimentally observed stripe AFM phase in real space. These hopping parameters are then used to study the ground-state properties of the semiconductor in momentum space. It is found to be a strongly correlated system with a large on-site Coulomb repulsion U, similar to the AFM Mott insulator — the parent compound of copper oxide superconductors. We also find that the electronic occupation numbers and magnetizations in the d_{xz} and d_{yz} orbitals become different simultaneously when $U > U_c$ (∼3.4 eV), indicating orbital ordering. These results imply that the rotational symmetry between the two orbitals is broken by orbital ordering and thus drives the strong anisotropy of the magnetic coupling that has been observed by experiments and that the stripe-type AFM order in this compound may be caused by orbital ordering together with the observed large anisotropy.

Keywords iron-based superconductor, two-orbital model, stripe AFM phase, rhombus Fe vacancy order, orbital ordering

PACS numbers 74.70.Xa, 75.25.Dk, 71.27.+a, 71.30.+h

1 Introduction

Recently, the discovery of superconductivity in the alkali metal iron selenides $A_xFe_{2-y}Se_2$ (where A = K, Cs, Tl/K, or Rb) [1–4], which have the same structure as the 122-type iron pnictides $BaFe_2As_2$, has stimulated great interest in the study of iron-based superconductors. Because the critical temperature T_c of these materials is above 30 K, comparable to that of the iron pnictides, plus the fact that some of them are magnetic insulators, their study may serve as a connection between the iron and copper superconductors [5].

In addition, they exhibit many novel properties that the cuprates and iron pnictides do not have [6]. For example, angle-resolved photoemission spectroscopy (ARPES) experiments display only electron-like pockets at $(\pi, 0)$ and $(0, \pi)$ points on the Fermi surface [7–9]. The absence of hole pockets seems to contradict the belief that Fermi surface nesting between electron and hole pockets is crucial for antiferromagnetic (AFM) order and superconducting pairing [10, 11], which is a widely held view for iron pnictides. Phase separation is also observed in many measurements, for example, from scanning tunneling microscopy and ARPES [12–14].

Another exotic phenomenon of the compounds $A_xFe_{2-y}Se_2$ is that there are different types of Fe vacancy orders, depending on the degree of doping. Since the report of a $\sqrt{5} \times \sqrt{5}$ Fe vacancy order with an exotic block AFM order, a novel large magnetic moment ($3.31\mu_B$/Fe), and a unique high Néel transition temperature (559 K) [15], and the subsequent finding that superconductivity occurs with a highly ordered $\sqrt{5} \times \sqrt{5}$ block AFM order [16], various compounds with iron vacancy orders as well as magnetic orders have been widely studied both experimentally and theoretically. For example, neutron diffraction studies on semiconducting $K_{0.85}Fe_{1.54}Se_2$ reveal a rhombus Fe vacancy order

and stripe-type AFM order [17]. The observed magnetic order is the same as that of the iron pnictide parent compounds, but the magnetic moment ($\approx 2.8\mu_B$) and Néel temperature (280 K) are much higher. Because the superconductivity emerges when the stripe AFM order is suppressed, it is conjectured that the new semiconducting stripe AFM phase is the true parent phase of the alkali metal iron selenide superconductors. Moreover, a recent neutron scattering study on the isomorphous Se compound $Rb_{0.8}Fe_{1.5}S_2$ also revealed a semiconducting phase with stripe-type AFM order and rhombus vacancy order [18]. In addition, the values of the magnetic moment and Néel temperature are nearly the same as previously observed in $K_{0.85}Fe_{1.54}Se_2$. These findings have prompted the belief that the stripe AFM order originates from local strong electron correlations rather than from the weak coupling of Fermi surface nesting. Furthermore, strong anisotropic magnetic couplings are also observed in both of these compounds, because the spin waves observed experimentally can be described accurately by an effective Heisenberg model with sign-changing anisotropic electron interactions in the *ab* plane [19, 20]. It has therefore been concluded that such strong anisotropy of the magnetic coupling may arise from orbital ordering.

Because the AFM spin fluctuations are strongly related to electron pairing and superconductivity, the determination of the origin of the magnetism and magnetic interactions is the key to understanding the superconductivity. In this paper, we will use the minimal two-orbital Hubbard model to investigate the rhombus Fe vacancy order with stripe AFM order both in real space and momentum space. The magnetic order and the Fe vacancy order from the two-orbital Hubbard model in real space are in good agreement with those observed by neutron scattering. We find that, although the next-next-nearest-neighbor (NNNN) hopping parameters are very small, they are, nonetheless, very important for the presence of the stripe AFM order. We then use the parameters obtained in real space to study the ground state properties of the semiconducting $KFe_{1.5}Se_2$ in momentum space. Based on our results, we discuss briefly the microscopic origin of the stripe-type AFM order and the physical picture that properly describes the alkali metal iron selenide $A_xFe_{2-y}Se_2$ superconductors.

2 Model and techniques

2.1 Model Hamiltonian

In this paper, we will use the two-orbital Hubbard model based on d_{xz} and d_{yz} orbitals, which have been shown to give the dominant contribution to the Fermi surface [21]. This is the simplest multiorbital model for the iron-based superconductors but can reveal the essential low-energy physics behavior. The two-orbital model can also be used to study other superconductors, such as the BiS_2 layered superconductor [22].

The Hamiltonian for a two-orbital Hubbard model generally contains two parts, namely, the tight-binding term and the on-site Coulombic interaction term, and is given by

$$H = H_{\rm TB} + H_{\rm int}. \tag{1}$$

The rhombus iron vacancies lead to a supercell as shown in Fig. 1(a). The tight-binding term in momentum space is defined as

$$H_{\rm TB} = \sum_{\boldsymbol{k},\boldsymbol{i},\boldsymbol{j},\alpha,\beta,\sigma} \xi^{\alpha,\beta}_{\boldsymbol{i},\boldsymbol{j}}(\boldsymbol{k}) c^{\dagger}_{\boldsymbol{i},\alpha,\sigma}(\boldsymbol{k}) c_{\boldsymbol{j},\beta,\sigma}(\boldsymbol{k}), \tag{2}$$

where $c^{\dagger}_{\boldsymbol{i},\alpha,\sigma}$ creates an electron at site $\boldsymbol{i}$ [as labeled in Fig. 1(a)] with spin σ on an α orbital (and $\alpha = xz$ and yz stand for the d_{xz} and d_{yz} orbitals, respectively), $\xi^{\alpha,\beta}_{\boldsymbol{i},\boldsymbol{j}}(\boldsymbol{k}) = \sum t^{\alpha,\beta}_{\boldsymbol{i},\boldsymbol{j}} \exp[\boldsymbol{ik}\cdot(\boldsymbol{r}_j - \boldsymbol{r}_i)]$, with $t^{\alpha,\beta}_{\boldsymbol{i},\boldsymbol{j}}$ being the hopping amplitudes, and $\boldsymbol{k}$ is defined within the Brillouin zone of the supercell. For simplicity, we use t_1 to t_6 to represent $t^{\alpha,\beta}_{\boldsymbol{i},\boldsymbol{j}}$, as illustrated in Fig. 1(b).

The Coulombic interaction term at each site is given by

$$\begin{aligned} H_{\rm int} = {} & U \sum_{\boldsymbol{i},\alpha} n_{\boldsymbol{i},\alpha,\uparrow} n_{\boldsymbol{i},\alpha,\downarrow} + (U' - J/2) \sum_{\boldsymbol{i},\alpha<\beta} n_{\boldsymbol{i},\alpha} n_{\boldsymbol{i},\beta} \\ & -2J \sum_{\boldsymbol{i},\alpha<\beta} \boldsymbol{S}_{\boldsymbol{i},\alpha} \cdot \boldsymbol{S}_{\boldsymbol{i},\beta} \\ & +J' \sum_{\boldsymbol{i},\alpha<\beta} \left(c^{\dagger}_{\boldsymbol{i},\alpha,\uparrow} c^{\dagger}_{\boldsymbol{i},\alpha,\downarrow} c_{\boldsymbol{i},\beta,\downarrow} c_{\boldsymbol{i},\beta,\uparrow} + \text{H.c.} \right), \end{aligned} \tag{3}$$

where $\boldsymbol{S}_{\boldsymbol{i},\alpha}$ ($n_{\boldsymbol{i},\alpha}$) corresponds to the spin (electronic density) of orbital α at site $\boldsymbol{i}$, and $n_{\boldsymbol{i},\alpha} = n_{\boldsymbol{i},\alpha,\uparrow} + n_{\boldsymbol{i},\alpha,\downarrow}$. These terms refer to, respectively, an on-site intraorbital Hubbard repulsion U, an on-site interorbital repulsion U' satisfying $U' = U - 2J$ by rotational invariance, and a finite Hund's coupling J. In brief, the first term describes a Hubbard on-site repulsion for the electrons located in the same orbital, the second term is the on-site interorbital repulsion for the electrons located in different orbitals, and the third term is a Hund term with a ferromagnetic coupling J. The pair-hopping interaction is given by the fourth term, and its coupling $J' = J$ is obtained by symmetry. All of the following studies are based on this two-orbital Hubbard model.

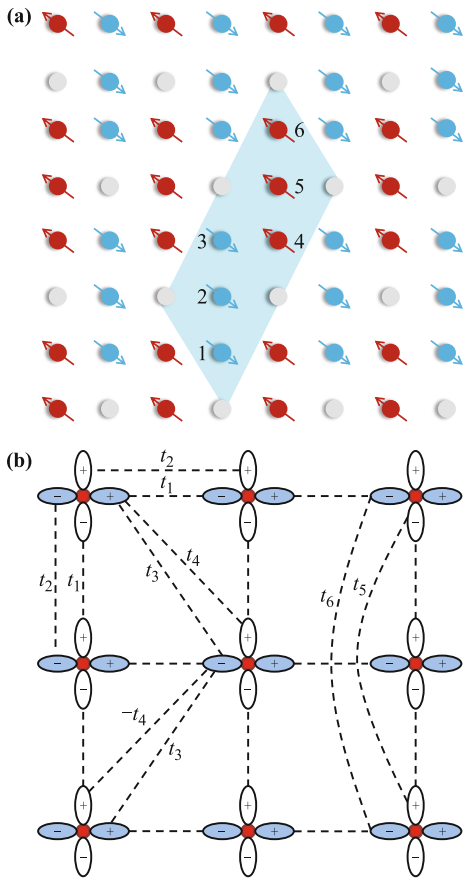

Fig. 1 **(a)** Sketch of the rhombus Fe vacancy order and the stripe type magnetic order of the semiconducting $KFe_{1.5}Se_2$. The gray circles are represent the Fe vacancies. The blue dashed area marks the unit cell that contains 6 Fe atoms and 2 Fe vacancies. **(b)** The hopping parameters of the two-orbital model on a Fe square lattice. The projections of the d_{xz} (d_{yz}) orbital onto the xy plane are depicted in blue (white); t_1, t_2, t_3, and t_4 are the same as in Ref. [23]; we also show the NNNN hopping amplitude t_5 (t_6) between the σ-orbital (π-orbital).

2.2 Mean-field approximation

To study the ground state properties of the stripe AFM phase with the rhombus iron vacancy order, a mean-field approximation is applied to the Hamiltonian. As a standard procedure, only the mean-field values for the diagonal operators are considered; these can be written as

$$\langle c^{\dagger}_{\boldsymbol{i},\alpha,\sigma} c_{\boldsymbol{i},\beta,\sigma'} \rangle = \left[n_{\boldsymbol{i},\alpha} + \frac{\sigma}{2} \cos\left(\boldsymbol{q}\cdot\boldsymbol{r}_{\boldsymbol{i}}\right) m_{\boldsymbol{i},\alpha} \right] \delta_{\alpha\beta}\delta_{\sigma\sigma'}, \tag{4}$$

where $\sigma = \pm 1$ corresponds to up and down spins, respectively, $\boldsymbol{q}$ is the magnetic order wave vector of the ground state, and $n_{\boldsymbol{i},\alpha}$ and $m_{\boldsymbol{i},\alpha}$ describe, respectively, the electronic density and magnetization in orbital α at site $\boldsymbol{i}$, which can be calculated self-consistently. Applying Eq. (4) to $H_{\rm int}$, we can derive the mean-field interaction Hamiltonian in momentum space as

$$H^{\rm MF}_{\rm int} = \sum_{\boldsymbol{k},\boldsymbol{i},\alpha,\sigma} [\epsilon_{\boldsymbol{i},\alpha} c^{\dagger}_{\boldsymbol{k},\boldsymbol{i},\alpha,\sigma} c_{\boldsymbol{k},\boldsymbol{i},\alpha,\sigma} + \eta_{\boldsymbol{i},\alpha,\sigma} (c^{\dagger}_{\boldsymbol{k},\boldsymbol{i},\alpha,\sigma} c_{\boldsymbol{k}+\boldsymbol{q},\boldsymbol{i},\alpha,\sigma} + \text{H.c.})] + C, \tag{5}$$

where

$$\epsilon_{\boldsymbol{i},\alpha} = U n_{\boldsymbol{i},\alpha} + (2U' - J) \sum_{\beta\neq\alpha} n_{\boldsymbol{i},\beta},$$

$$\eta_{\boldsymbol{i},\alpha,\sigma} = -\frac{\sigma}{2} \left(U m_{\boldsymbol{i},\alpha} + J \sum_{\beta\neq\alpha} m_{\boldsymbol{i},\beta} \right).$$

The last term of Eq. (5) is a constant given by

$$C = -NU \sum_{\boldsymbol{i},\alpha} \left(n^2_{\boldsymbol{i},\alpha} - \frac{1}{4} m^2_{\boldsymbol{i},\alpha} \right) - N(2U' - J) \sum_{\boldsymbol{i},\alpha\neq\beta} n_{\boldsymbol{i},\alpha} n_{\boldsymbol{i},\beta} + \frac{NJ}{2} \sum_{\boldsymbol{i},\alpha\neq\beta} m_{\boldsymbol{i},\alpha} m_{\boldsymbol{i},\beta},$$

where N is the number of sites.

The full mean-field Hamiltonian $H^{\rm MF} = H_{\rm TB} + H^{\rm MF}_{\rm int}$ is quadratic; thus, it can be numerically solved for a fixed set of mean-field parameters by using the standard library subroutines. The orbital electronic occupation number $n_{\boldsymbol{i},\alpha}$ and magnetization $m_{\boldsymbol{i},\alpha}$ are obtained self-consistently by minimizing the energy via an iterative procedure. During the iterations, $\sum_{\alpha} n_{\boldsymbol{i},\alpha}$ is fixed at each step; namely, the total electronic density is a constant at each Fe site. The reader should assume that these are the electronic densities for this model throughout the manuscript, and we can change their values conveniently in a parameter input file. Thus, we can easily study the ground state properties of $KFe_{1.5}Se_2$ for different doping levels. The numerical solution of the mean-field Hamiltonian allows us to calculate $m_{\boldsymbol{i},\alpha}$ and $n_{\boldsymbol{i},\alpha}$ at a particular magnetic order wave vector $\boldsymbol{q}$. Here, we fix $\boldsymbol{q}$ at $(\pi, 0)$ to investigate the stripe-type AFM order. Although all the Fe $3d$ orbitals should be considered for more accurate results, the simple two-orbital Hubbard model introduced above can provide qualitatively correct results for the ground state properties.

2.3 Hopping parameters

The hopping parameters are obtained by finding the stripe-type AFM phase on an 8×8 cluster with rhombus Fe vacancies, as sketched in Fig. 2(b), using periodic boundary conditions. Here we use the standard real space two-orbital Hubbard model. This model has been extensively studied by our group and others [24, 25]. More

specifically, the real space two-orbital Hubbard model used here is the same as in Ref. [26]. Earlier studies indicated that this model has a Fermi surface at $U = 0$, in agreement with band-structure results for pnictides without considering the NNNN interactions and Fe vacancies [24]. In our model, we introduce both the NNNN interactions and rhombus Fe vacancy order. To compare with other iron superconductor materials, we set the in-plane nearest-(t_1 and t_2), next-nearest-(t_3 and t_4) neighbor hopping amplitudes to be the same as the classical two-orbital hopping parameters [23], which are widely used in the study of iron pnictide superconductors.

In our research, it is very hard to obtain a stripe-type magnetic order unless t_5 and t_6 are included in the model, as shown in Fig. 2(a). Therefore, we speculate that the NNNN hopping parameters are very small; nonetheless, they are important to the emergence of the stripe-type AFM order. This discovery is consistent with a previous study in which inelastic neutron scattering was used to study block AFM order spin waves in the insulating compound $Rb_{0.89}Fe_{1.58}Se_2$ [27]. There, the authors use a Heisenberg model with anisotropic electron interactions to analyze the experimental results, concluding that the existence of NNNN superexchange couplings are very important, as they allow them to fit the entire spin wave spectra. An extended J_1–J_2–J_3 model also indicates that a third nearest neighbor AFM J_3 is necessary to describe the magnetic orders of the iron chalcogenides FeTe and $K_{0.8}Fe_{1.6}Se_2$ [28]. Our results combined with theirs lead to the conclusion that the inclusion of NNNN interactions in the Fe vacancy system makes it more realistic.

We obtain the stripe-type AFM order as shown in Fig. 2(b) through adjusting the NNNN hopping amplitudes (t_5 and t_6) and the on-site intraorbital repulsion U in a self-consistent procedure. The initial configurations for the calculations are chosen to be random, and the energy minimization results are obtained self-consistently. Therefore, the initial configurations for the iterations to search for the magnetic phase should be unbiased. We find that the resulting magnetic phase is in good agreement with the neutron diffraction measurements [17, 18]. In short, the set of hopping parameters we have obtained here are reasonable and can qualitatively capture the essential physics for a system with a rhombus Fe vacancy order and stripe-type AFM order. All the momentum space results below are based on this set of hopping parameters.

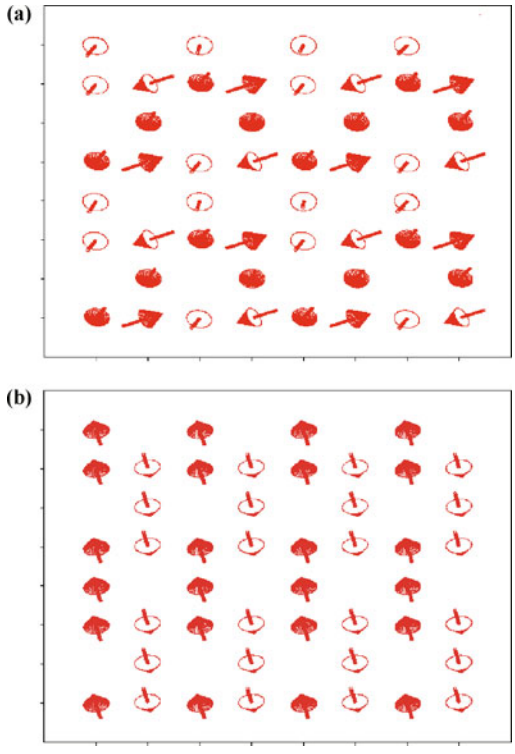

Fig. 2 The magnetic states of $KFe_{1.5}Se_2$ on an 8×8 cluster with rhombus Fe vacancy order. The hopping amplitudes are: $t_1 = -1.0$, $t_2 = 1.3$, $t_3 = t_4 = -0.85$ for all the results but $t_5 = t_6 = 0$ for **(a)** and $t_5 = -0.09$, $t_6 = 0.1$ for **(b)**. The electronic density $n = 2.1$, $U = 3.6$, $J/U = 0.3$.

3 Results

We first plot the total magnetization $m = \sum_\alpha m_{i,\alpha}$ as a function of the Coulomb repulsion U, as shown in Fig. 3. We observe that m becomes nonzero at a particular value of U_0. According to our study on band structure, the valence and conduction bands start to separate at nearly the same particular value of U_0, but, overall, some bands still overlap with each other and the chemical potential crosses both of them. Thus, the magnetic order has developed, but the system is still in a metallic phase. As we increase U further, the system develops into a semiconducting phase and the overlap between the bands vanishes. Finally, when U is large enough, the system becomes an insulator. We choose a large Hubbard U coupling strength to describe $KFe_{1.5}Se_2$, because it is a semiconductor. This is different from previous studies, in which a weak or intermediate Hubbard U is used to describe their systems under the same model but without iron vacancies for the pnictides [29]. Our results suggest that the stripe AFM semiconducting $KFe_{1.5}Se_2$ has local strong correlations; namely, the local electrons play a crucial role while the itinerant electrons may be irrelevant. This is similar to the case of AFM Mott insulator, which is the parent compound of copper oxide superconductors. Based on the present study, such strong AFM correlations may be caused by orbital ordering, which is

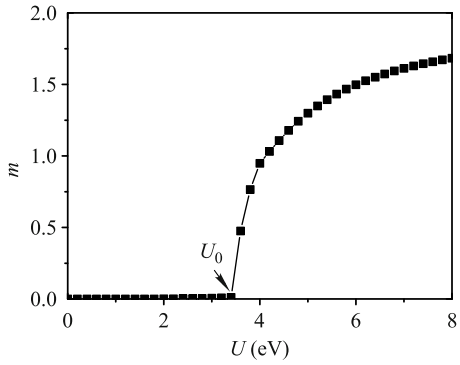

Fig. 3 The total $(\pi, 0)$ ordered magnetization m as a function of the Coulomb repulsion U (in eV units) for $J/U = 0.3$, $n = 2.1$.

consistent with our results, as shown in Fig. 4.

From Figs. 4(a) and (c), we find that the average electronic occupation numbers and magnetic moments of the d_{xz} and d_{yz} orbitals are entangled at half-filling ($n = 2.0$); we cannot distinguish the two orbitals and hence there is no orbital order. However, for $n = 2.1$, we can see from Fig. 4(b) that n_{xz} is larger than n_{yz} when $U > U_c$, whereas in Fig. 4(d) m_{xz} becomes smaller than m_{yz} at the same U_c, indicating the existence of orbital order in this case. Clearly, there seems to be an inverse relationship between the orbital magnetization and the orbital occupation. Although it is unclear whether the difference in orbital magnetization leads to the difference in orbital occupation, or *vice versa*, one thing is certain: The magnetizations of the d_{xz} and d_{yz} orbitals deviate from each other simultaneously at the same critical U_c where the orbital order appears. In this case, the rotational symmetry between the two orbitals is broken by the orbital ordering.

In addition to the results shown in Fig. 4, we have calculated the values of $n_{\boldsymbol{i},\alpha}$ and $m_{\boldsymbol{i},\alpha}$ for different degrees of doping, and found that the orbital order exists provided $n > 2.0$. Since large in-plane anisotropic magnetic couplings are found in this material by experiments [19] and via first-principles calculations [30], and they may be derived from the broken symmetry in the orbital degree of freedom [31], those dopings that lead to orbital symmetry being broken may be close to the real material. In this paper, we choose the electronic density $n = 2.1$ as a representative value for displaying and analyzing the results because the orbital order can be obtained at a relatively reasonable U_c, which is consistent with experiments.

From the discussions above we can speculate that the inclusion of the rhombus Fe vacancy order breaks the degeneracy of the d_{xz} and d_{yz} orbitals, just as found in earlier studies of the $\sqrt{5} \times \sqrt{5}$ Fe vacancy order in the same compound but with different doping values [32]. Because the spin and orbital are entangled, it is hard

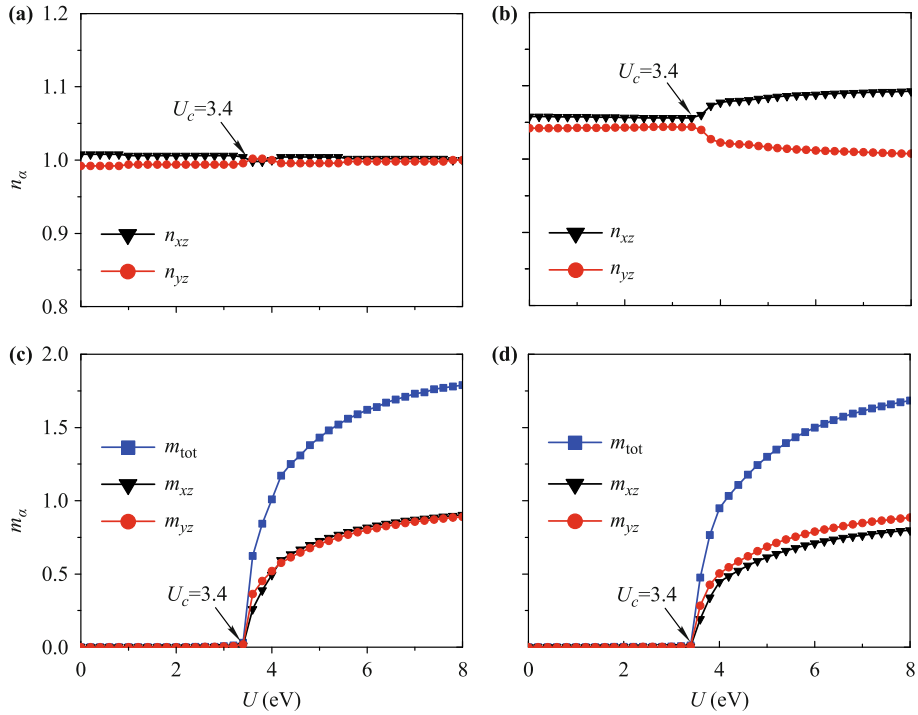

Fig. 4 The average orbital electronic occupation number n_α as a function of the Coulomb repulsion U for **(a)** $n = 2.0$ and **(b)** $n = 2.1$, respectively. The average orbital magnetization m_α as a function of the Coulomb repulsion U for **(c)** $n = 2.0$ and **(d)** $n = 2.1$, respectively. All the results are obtained with a mean-field approximation. The lattice size is 48×48 with periodic boundary conditions, and $J/U = 0.3$.

to say which one is the main degree of freedom. Our model analyses and experimental evidence indicates that the orbital degree of freedom could be an important factor for the experimentally observed anisotropy of magnetic coupling. In this case, the orbital order may give rise to the stripe AFM phase for the rhombus Fe vacancy order.

4 Discussion and conclusions

In summary, we have studied the two-orbital Hubbard model with mean-field approximation techniques, and the phase diagram for the semiconducting $KFe_{1.5}Se_2$ has been investigated in terms of the orbital magnetization and electronic occupation number as a function of the Coulomb repulsion U. Real materials could be described more accurately by including more orbitals, such as in the three- and five-orbital models, but this would be too complicated for calculations. By adjusting the electronic density in the two-orbital model, the physical properties of this compound can be studied qualitatively just as well as three- and five-orbital models. The electronic density n is taken to be 2.1 as a representative value to describe the real materials. The hopping parameters are obtained through searching for the experimentally observed stripe AFM order in real space [17, 18]. Although the NNNN hopping parameters are very small, they have noticeable contribution to the presence of the stripe AFM phase. The ground state properties of this material are then studied in momentum space using these hopping parameters. The total magnetic moment phase suggests that this compound is a system with strong local correlations similar to the AFM Mott insulators.

We also find that the magnetizations and electronic occupation numbers in d_{xz} and d_{yz} orbitals deviate from each other significantly at the same critical U_c, demonstrating the emergence of the orbital order. From these, we infer that the rhombus Fe vacancies enhance the electron correlation and break the degeneracy of the d_{xz} and d_{yz} orbitals. The orbital order may then lead to the strongly anisotropic magnetic couplings observed in $KFe_{1.5}Se_2$ and in recently measured $Rb_{0.8}Fe_{1.5}S_2$, as a result of rotational symmetry being broken. This prediction is compatible with first-principles calculations and inelastic neutron scattering observations [19, 30]. In short, the stripe-type AFM phase in $KFe_{1.5}Se_2$ and $Rb_{0.8}Fe_{1.5}S_2$ may originate from orbital ordering.

Acknowledgements We would like to thank Wei-Feng Tsai, Yao-Tai Kang, Qinlong Luo, and Weicheng Lv for useful discussions. This work was supported by the National Basic Research Program of China (Grant No. 2012CB821400), the National Natural Science Foundation of China (Grant Nos. 11574404 and 11275279), the Natural Science Foundation of Guangdong Province (Grant No. 2015A030313176), the National Supercomputer Center in Guangzhou, and the Fundamental Research Funds for the Central Universities of China.

References

1. J. G. Guo, S. F. Jin, G. Wang, S. C. Wang, K. X. Zhu, T. T. Zhou, M. He, and X. L. Chen, Superconductivity in the iron selenide $K_xFe_2Se_2$ ($0 \leqslant x \leqslant 1.0$), *Phys. Rev. B* 82(18), 180520 (2010)
2. A. Krzton-Maziopa, Z. Shermadini, E. Pomjakushina, V. Pomjakushin, M. Bendele, A. Amato, R. Khasanov, H. Luetkens, and K. Conder, Synthesis and crystal growth of $Cs_{0.8}(FeSe_{0.98})_2$: A new iron-based superconductor with T_c= 27 K, *J. Phys.: Condens. Matter* 23(5), 052203 (2011)
3. H. D. Wang, C. H. Dong, Z. J. Li, Q. H. Mao, S. S. Zhu, C. M. Feng, H. Q. Yuan, and M. H. Fang, Superconductivity at 32 K and anisotropy in $Tl_{0.58}Rb_{0.42}Fe_{1.72}Se_2$ crystals, *Europhys. Lett.* 93(4), 47004 (2011)
4. A. F. Wang, J. J. Ying, Y. J. Yan, R. H. Liu, X. G. Luo, Z. Y. Li, X. F. Wang, M. Zhang, G. J. Ye, P. Cheng, Z. J. Xiang, and X. H. Chen, Superconductivity at 32 K in single-crystalline $Rb_xFe_{2-y}Se_2$, *Phys. Rev. B* 83, 060512(R) (2011)
5. E. Dagotto, *Colloquium*: The unexpected properties of alkali metal iron selenide superconductors, *Rev. Mod. Phys.* 85(2), 849 (2013)
6. M. Guidry and Y. Sun, Superconductivity and superfluidity as universal emergent phenomena, *Front. Phys.* 10(4), 107404 (2015)
7. Y. Zhang, L. X. Yang, M. Xu, Z. R. Ye, F. Chen, C. He, H. C. Xu, J. Jiang, B. P. Xie, J. J. Ying, X. F. Wang, X. H. Chen, J. P. Hu, M. Matsunami, S. Kimura, and D. L. Feng, Nodeless superconducting gap in $A_xFe_2Se_2$ (A=K,Cs) revealed by angle-resolved photoemission spectroscopy, *Nat. Mater.* 10(4), 273 (2011)
8. T. Qian, X. P. Wang, W. C. Jin, P. Zhang, P. Richard, G. Xu, X. Dai, Z. Fang, J. G. Guo, X. L. Chen, and H. Ding, Absence of a holelike fermi surface for the iron-based $K_{0.8}F_{1.7}Se_2$ superconductor revealed by angle-resolved photoemission spectroscopy, *Phys. Rev. Lett.* 106(18), 187001 (2011)
9. X. P. Wang, T. Qian, P. Richard, P. Zhang, J. Dong, H. D. Wang, C. H. Dong, M. H. Fang, and H. Ding, Strong nodeless pairing on separate electron Fermi surface sheets in (Tl, K)$Fe_{1.78}Se_2$ probed by ARPES, *Europhys. Lett.* 93(5), 57001 (2011)
10. F. J. Ma and Z. Y. Lu, Iron-based layered compound LaFeAsO is an antiferromagnetic semimetal, *Phys. Rev. B* 78(3), 033111 (2008)
11. J. Dong, H. J. Zhang, G. Xu, Z. Li, G. Li, W. Z. Hu, D. Wu, G. F. Chen, X. Dai, J. L. Luo, Z. Fang, and N. L.

Wang, Competing orders and spin-density-wave instability in La($O_{1-x}F_x$)FeAs, *Europhys. Lett.* 83(2), 27006 (2008)

12. F. Chen, M. Xu, Q. Q. Ge, Y. Zhang, Z. R. Ye, L. X. Yang, J. Jiang, B. P. Xie, R. C. Che, M. Zhang, A. F. Wang, X. H. Chen, D. W. Shen, J. P. Hu, and D. L. Feng, Electronic identification of the parental phases and mesoscopic phase separation of $K_xFe_{2-y}Se_2$ superconductors, *Phys. Rev. X* 1(2), 021020 (2011)
13. A. Ricci, N. Poccia, G. Campi, B. Joseph, G. Arrighetti, L. Barba, M. Reynolds, M. Burghammer, H. Takeya, Y. Mizuguchi, Y. Takano, M. Colapietro, N. L. Saini, and A. Bianconi, Nanoscale phase separation in the iron chalcogenide superconductor $K_{0.8}Fe_{1.6}Se_2$ as seen via scanning nanofocused X-ray diffraction, *Phys. Rev. B* 84, 060511(R) (2011)
14. D. X. Mou, L. Zhao, and X. J. Zhou, Structural, magnetic and electronic properties of the iron-chalcogenide $A_xFe_{2-y}Se_2$ (A=K, Cs, Rb, and Tl, etc.) superconductors, *Front. Phys.* 6(4), 410 (2011)
15. W. Bao, Q. Z. Huang, G. F. Chen, M. A. Green, D. M. Wang, J. B. He, and Y. M. Qiu, A novel large moment antiferromagnetic order in $K_{0.8}Fe_{1.6}Se_2$ superconductor, *Chin. Phys. Lett.* 28(8), 086104 (2011)
16. W. Bao, G. N. Li, Q. Z. Huang, G. F. Chen, J. B. He, D. M. Wang, M. A. Green, Y. M. Qiu, J. L. Luo, and M. M. Wu, Superconductivity tuned by the iron vacancy order in $K_xF_{2-y}Se_2$, *Chin. Phys. Lett.* 30(2), 027402 (2013)
17. J. Zhao, H. Cao, E. Bourret-Courchesne, D. H. Lee, and R. J. Birgeneau, Neutron-diffraction measurements of an antiferromagnetic semiconducting phase in the vicinity of the high-temperature superconducting state of $K_xFe_{2-y}Se_2$, *Phys. Rev. Lett.* 109(26), 267003 (2012)
18. M. Wang, W. Tian, P. Valdivia, S. X. Chi, E. Bourret-Courchesne, P. C. Dai, and R. J. Birgeneau, Two spatially separated phases in semiconducting $Rb_{0.8}Fe_{1.5}S_2$, *Phys. Rev. B* 90(12), 125148 (2014)
19. J. Zhao, Y. Shen, R. J. Birgeneau, M. Gao, Z. Y. Lu, D. H. Lee, X. Z. Lu, H. J. Xiang, D. L. Abernathy, and Y. Zhao, Neutron scattering measurements of spatially anisotropic magnetic exchange interactions in semiconducting $K_{0.85}Fe_{1.54}Se_2$ ($T_N = 280$ K), *Phys. Rev. Lett.* 112(17), 177002 (2014)
20. M. Wang, P. Valdivia, J. X. Chen, W. L. Zhang, R. A. Ewings, T. G. Perring, Y. Zhao, L. W. Harriger, J. W. Lynn, E. Bourret-Courchesne, D. H. Lee, D. X. Yao, and R. J. Birgeneau, Spin waves and spatially anisotropic exchange interactions in the $S = 2$ stripe antiferromagnet $Rb_{0.8}Fe_{1.5}S_2$, *Phys. Rev. B* 92, 041109(R) (2015)
21. L. Boeri, O. V. Dolgov, and A. A. Golubov, Is $LaFeAsO_{1-x}F_x$ an electron-phonon superconductor? *Phys. Rev. Lett.* 101(2), 026403 (2008)
22. Y. Liang, X. X. Wu, W. F. Tsai, and J. P. Hu, Pairing symmetry in layered BiS_2compounds driven by electron-electron correlation, *Front. Phys.* 9(2), 194 (2014)
23. S. Raghu, X.-L. Qi, C.-X. Liu, D. J. Scalapino, and S.-C. Zhang, A minimal two-band model for the superconducting Fe-pnictides, *Phys. Rev. B* 77, 220503(R) (2008)
24. M. Daghofer, A. Moreo, J. A. Riera, E. Arrigoni, D. J. Scalapino, and E. Dagotto, Model for the magnetic order and pairing channels in Fe pnictide superconductors, *Phys. Rev. Lett.* 101(23), 237004 (2008)
25. Q. Jiang, Y. T. Kang, and D. X. Yao, Spin, charge, and orbital orderings in iron-based superconductors, *Chin. Phys. B* 22(8), 087402 (2013)
26. Q. L. Luo, D. X. Yao, A. Moreo, and E. Dagotto, Charge stripes in the two-orbital Hubbard model for iron pnictides, *Phys. Rev. B* 83(17), 174513 (2011)
27. M. Wang, C. Fang, D. X. Yao, G. Tan, L. W. Harriger, Y. Song, T. Netherton, C. Zhang, M. Wang, M. B. Stone, W. Tian, J. Hu, and P. Dai, Spin waves and magnetic exchange interactions in insulating $Rb_{0.89}Fe_{1.58}Se_2$, *Nat. Commun.* 2, 580 (2011)
28. W. Li, C. Setty, X. H. Chen, and J. P. Hu, Electronic and magnetic structures of chain structured iron selenide compounds, *Front. Phys.* 9(4), 465 (2014)
29. R. Yu, K. T. Trinh, A. Moreo, M. Daghofer, J. A. Riera, S. Haas, and E. Dagotto, Magnetic and metallic state at intermediate Hubbard U coupling in multiorbital models for undoped iron pnictides, *Phys. Rev. B* 79(10), 104510 (2009)
30. X. W. Yan, M. Gao, Z. Y. Lu, and T. Xiang, Electronic structures and magnetic order of ordered-Fe-vacancy ternary iron selenides $TlFe_{1.5}Se_2$ and $AFe_{1.5}Se_2$ (A=K, Rb, or Cs), *Phys. Rev. Lett.* 106(8), 087005 (2011)
31. C. C. Lee, W. G. Yin, and W. Ku, Ferro-orbital order and strong magnetic anisotropy in the parent compounds of iron-pnictide superconductors, *Phys. Rev. Lett.* 103(26), 267001 (2009)
32. W. C. Lv, W. C. Lee, and P. Phillips, Vacancy-driven orbital and magnetic order in $(K,Tl,Cs)_yFe_{2-x}Se_2$, *Phys. Rev. B* 84(15), 155107 (2011)